Variation in Growth Forms of the Reef Coral *Montastrea annularis* (Ellis and Solander): A Quantitative Evaluation of Growth Response to Light Distribution Using Computer Simulation

Richard R. Graus
and Ian G. Macintyre

ABSTRACT

A new computer simulation model is used to evaluate the relationship between the various growth forms of small isolated colonies of *Montastrea annularis* (Ellis and Solander) and submarine light distribution. In this model (Model 2) calcification rate as a function of light intensity is calculated from detailed measurements of skeletal growth rate and skeletal density in colonies collected from various depths off Carrie Bow Cay, Belize, and one large colony from Discovery Bay, Jamaica. A previous model (Model 1) was based on laboratory studies of photosynthesis rates and calcification in response to light intensity (Graus and Macintyre, 1976).

Although these two models represent independent approaches to the understanding of coral morphogenesis, the simulation outputs are essentially similar and replicate the morphotypic variations of *M. annularis* observed in increasing water depths off Carrie Bow Cay. These two models together corroborate the hypothesis that light intensity and distribution provide the major ecological control for the skeletal morphogenesis of *M. annularis*.

Introduction

Numerous colonies of the Caribbean coral *Montastrea annularis* (Ellis and Solander) collected be-

Richard R. Graus and Ian G. Macintyre, *Department of Paleobiology, National Museum of Natural History, Smithsonian Institution, Washington, D.C. 20560.*

tween 1972 and 1979 from various reef settings and depths at Carrie Bow Cay, Belize, have provided considerable morphological information about skeletal growth and its intraspecific variability. Colonies of *M. annularis* transplanted from shallow water to deep water and vice versa helped us to identify skeletal characteristics that are light responsive. The modification of these characteristics in the transplanted colonies and their variability among in situ colonies suggest that ecophenotypic factors account for differences in growth form over the environmental range of this species, principally the ecophenotypic response of *M. annularis* to light. New data on light response have allowed us to propose a second model for skeletal growth that corroborates the hypothesis generated from an earlier model that was based on experiments of light-mediated photosynthesis and calcification of *M. annularis* (see Graus and Macintyre, 1976; Graus, 1977).

Methods

Between 1972 and 1979 colonies of *Montastrea annularis* were collected from various reef locations off Carrie Bow Cay over a depth of 0.5 to 30.0 m. Many of these colonies were stained—some annually over a period of five years—with Alizarin Red-S to provide an accurate time marker for measuring growth rate. Stain lines correlated with cyclic density bands in x-radiographs (Macintyre and Smith, 1974), which were also used to measure growth.

The effects of ambient radiance distribution on growth form were tested by transplanting colonies from shallow to deep locations on the reef and vice versa (details given in Table 34). First, however, each colony was stained with Alizarin Red-S and nails were hammered into the skeleton vertically at the crest and horizontally in the direction of North in order to establish the original orientation at the new site. The colony was removed with a hammer, cemented to a concrete block, transplanted, left for three years, and then collected.

Two-dimensional light fields were measured in the solar plane around several in situ and transplanted colonies at depths from 0.5 to 20.0 m by means of an underwater radiometer-photometer (United Detector Technology 40X Opto-Meter). Measurements were recorded on clear days at 30° intervals from 0° (up) to 180° (down), east and west of vertical, while the sun was near the zenith. Although we did not conduct a comprehensive survey of light at other azimuths and solar altitudes, we computed an attenuation coefficient that enabled us to correlate our Belizean data with the more extensive radiance data from Curaçao (Roos, 1967).

Morphological measurements were obtained from vertical skeletal slabs (approximately 0.5 cm thick) cut through the crest of each colony. The slabs were x-rayed and each negative made into a positive contact print on which morphological measurements were made directly. Consecutive dark and light density bands prominent in the x-radiographs represent annual skeletal growth in most colonies (Figure 185). Care must be taken, however, to differentiate between these pairs of bands and other bands caused by local and regional noncyclic environmental fluctuations. Skeletal growth rate was determined on the basis of the length of a corallite within a given band (since corallites normally grow perpendicular to the growth surface). This distance was measured with vernier calipers.

Skeletal growth rate is known to vary with orientation of the corallites, which can be determined by measuring the corallite growth angle. This angle is defined as the interior angle between a corallite's axis of growth and the vertical direction. We measured this angle with a straight edge and a goniometer.

Skeletal density was measured in rectangular slabs (approximately $3 \times 3 \times 1$ cm) cut from (a) the crest and flanks of 9 specimens of *Montastrea annularis* from Carrie Bow Cay and (b) 12 posi-

TABLE 34.—Transplant conditions for colonies of *Montastrea annularis*; all at Carrie Bow Cay reef except colonies 5 and 6 (P. Dustan's 3-year transplant colonies from Jamaica); colony 8 rotated 65° at same depth

Colony number	Original depth (m)	Transplant depth (m)	Transplant location	Transplant date	Collection date
1	1	14	Outer ridge	Jun 1975	Mar 1978
2	1	14	Outer ridge	Jun 1975	Mar 1978
3	1	21	Inner-reef slope	Apr 1975	Mar 1978
4	1	21	Inner-reef slope	Apr 1975	Mar 1978
5	1	31	Fore-reef slope	Jun 1975	Mar 1978
6	45	15	Jamaica	Aug 1972	Aug 1975
7	45	15	Jamaica	Aug 1972	Aug 1975
8	1	1	Back reef	Apr 1975	Mar 1978

FIGURE 185—Variations of coral growth patterns of *Montastrea annularis* with respect to water depth along the Carrie Bow Cay transect as shown by the five morphotypes recognized in this study: *a*, hemisphere, 1 m; *b*, tapered hemisphere, 10 m; *c*, column, 22 m; *d*, flared column, 25 m; *e*, plate, 30 m; colonies are in life orientation, except for the plate (*e*), which originally dipped 30° to the left.

tions spanning the entire range of growth angles on a colony of *M. annularis* from a depth of 5 m off Jamaica. An analytical balance was used to weigh the slabs both in air (*Wa*) and suspended in water (*Ww*). The weight in water was recorded within seconds of immersion in order to minimize seepage into the skeleton. The percentage of error for this procedure was thereby kept to less than 1%. The weights in air and in water together with the density of water ($P_l = 1.000$ g/cm^3) were used to calculate skeletal density (P_s) from Archimedes' formulas as follows:

$$P_s = P_l \cdot \frac{Wa}{(Wa - Ww)}$$

Intercorallite spacing was measured on five colonies from depths of 0.5 to 30.0 m off Carrie Bow Cay and on one colony from a depth of 5 m off Jamaica. Photographic studies were based on enlarged 8 × 10 in (20 × 25 cm) prints of small sections of the surface of Carrie Bow Cay specimens, both at the crest and lower flanks of the colony. In the 30 m plate morphotype, however, sections at the center and outer edge were photographed. The specimen from Jamaica was photographed at 12 positions over the entire range of corallite growth angles. Owing to curvature of the surface of colonies, only 10 to 15 corallites at the center of each print were oriented perpendicular to the film and therefore only those could be measured without a distortion of distance. The distance between the centers of each neighboring pair of these central corallites was measured with vernier callipers.

Results

MORPHOLOGICAL VARIABILITY.—The massive variety of *Montastrea annularis* has been classified into three morphotypes on the basis of variations that occur at different depths over the entire range of this species: hemispheric, 0–5 m; columnar, 5–25 m; and platy, >25 m (Macintyre and Smith, 1974; Graus and Macintyre, 1976; Graus, 1977). Our recent measurements of specimens from Carrie Bow Cay indicate that these three morphotypic stages are actually part of a contin-

uous gradient that changes with depth. This gradient is described below in terms of five colonies that reflect distinct morphotypic stages.

Hemisphere (Figure 185*a*): The colony from a depth of 1 m in the rubble and pavement zone off Carrie Bow Cay shows 10 years of growth from its fractured base. Its predominant morphological features are radiating corallites and the almost concentric, paired, high and low density bands representing annual growth. The rate of skeletal growth was found to be highest at the crest, averaging 0.83 cm/y for the life of the colony. The rate is nearly constant for angles of corallite growth up to 60°, but gradually diminishes thereafter and reaches 0.24 cm/yr at the maximum angle of 141°. This pattern repeats annually, gradually developing the form of the corallum. This growth pattern also influences the directions of corallite growth. At the crest, where the growth rate is nearly constant, all corallites except for those lying along the vertical axis radiate linearly away from each other. Because of differential growth rate along the flanks, corallites curve away from the vertical until the polyps eventually die out at the lower periphery.

Interior budding occurs in regions of greatest corallite divergence (for example, the crest and raised humps). Peripheral budding occurs along the lower flanks at the free edge of the epitheca, and thus gradually extends the flanks to the substratum.

Tapered Hemisphere (Figure 185*b*): This specimen from a depth of 10 m in the high-relief spur and groove zone resembles the hemispheric form in its high, relatively uniform growth rate (0.93 cm/y) over the broad region of the crest. However, the maximum corallite growth angle at 110° is lower than that of the hemispheric form. The tapered form expands upward rapidly and outward gradually; because the maximum angle of corallite growth is greater than 90°, the mature form becomes a hemisphere that tapers like an inverted cone toward a smaller base.

Column (Figure 185*c*; Plate 4: *center left*): This specimen from a depth of 22 m on the inner-reef slope has a growth history of 24 years. Maximum skeletal growth rate at the crest averages 0.63

cm/y, which is lower than in either the hemisphere or tapered hemisphere stages. The growth rate diminishes beginning at a 10° angle of corallite growth and reaches a minimum rate of 0.18 cm/y at an angle of 95°. The high differential growth rate between the crest and flanks produces strong curvature and divergence of corallites and thus creates room for new buds. Almost all corallites in the colony originate in an area that was an earlier crest of the colony. The geometry of corallite growth paths and the shape of the entire colony are similar to the axial growth pattern of branching corals (for example, species of *Stylophora*, *Pocillopora*, *Porites*, and *Dendrogyra*). Peripheral budding at the lower flanks forms epithecal extensions of the lower flanks, or skirts that become separated from the main skeleton. Buds initially grow parallel to the surface of the skirt, but within a year or two these buds turn around to a nearly perpendicular orientation. The skirts develop a concave upward form after several years because each new generation of buds turns a few additional degrees toward the vertical. Because these buds are not locked in on all sides by other corallites, they have more freedom in their direction of growth and can thereby influence the shape and orientation of the skirt. Although the colony has become distinctly columnar after 24 years of growth, its annual bands indicate that the earliest stage was hemispherical and that the present columnar form developed gradually.

Flared Column (Figure 185d): This colony from 25 m indicates a maximum growth rate at the crest of 0.64 cm/y, which is similar to that of the columnar form, but here the maximum angle of corallite growth (60°) is much lower than for the columnar form. As in that form, peripheral budding in the flared column leads to the formation of skirts. The growth habit of this stage produces a broadly conical colony that is peaked at the crest and flared at the base.

Plate (Figure 185e): This colony from 30 m on the fore-reef slope shows 20 years of growth from the base. Although the colony's orientation is horizontal in this illustration, it was inclined 30° to the left during its life on the reef. Its average growth rate is 0.35 cm/y but at the maximum vertical angle (53°) growth rate is only 0.06 cm/y. Although interior budding is not evident in the x-radiograph of this colony, it has been observed in raised areas of this plate. Peripheral epithecal budding is dominant, however, and new corallites form in the same manner as they do on the skirts of the column and flared column morphotypes.

GENERAL TRENDS IN MORPHOLOGY WITH DEPTH.—*Maximum Growth Rate and Maximum Growth Angle:* Data (Figures 186, 187) from 38 colonies of *Montastrea annularis* on the maximum annual growth rate and maximum angle of corallite growth—the primary factors controlling form—indicate that the relationships with depth are probably continuous and linear. The least squares regression line in Figure 186 predicts a maximum skeletal growth rate of 0.9739 cm/y at 0 m depth and a minimum skeletal growth rate of 0 cm/y (that is, the cessation of growth) at 51 m. The regression line in Figure 187 predicts a 135.2° maximum angle of corallite growth at 0 m and a minimum angle of 0° at 50.6 m depth. The predicted maximum depth limit of about 50 m for both trends is about 10% greater than the 45 m maximum depth said to be normal for the species (Goreau and Wells, 1967).

As expected, maximum skeletal growth rate and maximum angle of corallite growth correlate positively and significantly with each other ($r = 0.689$, $p < 0.01$). Because the trends are covariant, morphotypes can be classified in terms of only one variable, that is, maximum angle of corallite growth:

Morphotype	Range of maximum angles (°)
Hemisphere	120–180
Tapered hemisphere	105–120
Column	75–105
Flared column	45–75
Plate	0–45

Despite the statistically significant linear depth trends, dispersion about each of the calculated lines is notable. At any given depth, specimens vary in both maximum growth rate and maximum angle of corallite growth as well as in growth form. These parameters also vary from year to year within a single colony (Figure 185).
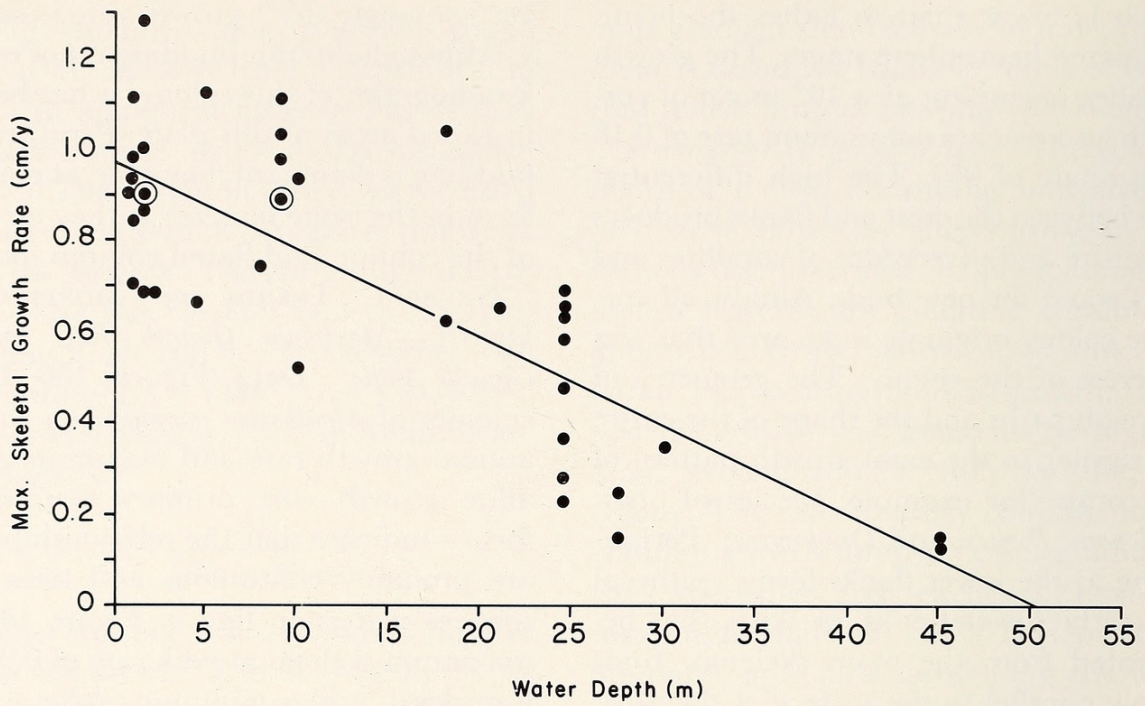
FIGURE 186.—Maximum skeletal growth rate at the crest of colonies of *Montastrea annularis* as a function of water depth, all data from Carrie Bow Cay transect except values from 45 m, Dancing Lady Reef, Jamaica (open circles with dots = duplicate values; regression equation is $Y = -0.019X + 0.9739$; linear correlation coefficient, $r = -0.729$, $P < 0.01$).
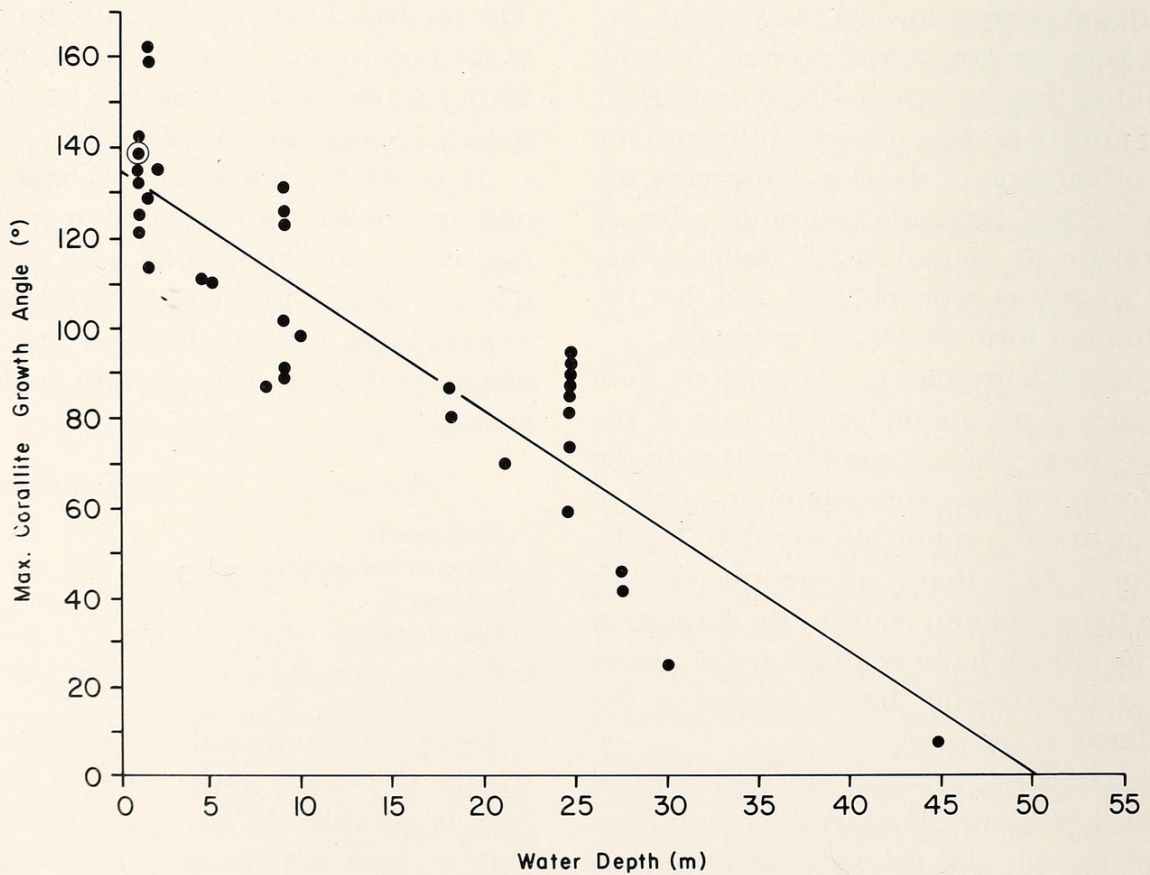

FIGURE 187.—Maximum corallite growth angle (with respect to vertical) as a function of water depth for colonies of *Montastrea annularis*, all data from Carrie Bow Cay except the 45 m value, Jamaica (regression equation is $Y = -2.700X + 135.156$; linear correlation coefficient, $r = -0.872$, $P < 0.01$).

Skeletal Density: The increase in skeletal density with depth is depicted in Figure 188. The regression equation predicts a minimum skeletal density of 1.5336 g/cm^3 at the surface that increases to 2.0856 g/cm^3 at a depth of 30 m. No relationship between skeletal density and corallite growth angle could be clearly established. In some colonies, density increases from the crest to the flanks but in others it does not. Our inability to demonstrate this effect—which is readily observable in x-radiographs (Figure 185) as an increase in the ratio of dark area (high density) to light area (low density)—may be due to the comparatively large size of the skeletal slabs being considered. Slabs taken from the lower flanks of a colony generally include portions of skeleton from a previous crest. This material probably masks any differences in density between crest and flanks. If significantly smaller slabs were used, however, measurement error due to water leakage into the skeleton would be unacceptably magnified.

Intercorallite Spacing: The increased intercorallite spacing at the crest with increasing depth is plotted in Figure 189. The trend in mean spacing concurs with Dustan's data (1975), although our results are not directly comparable with his because of unit differences. Our values of minimum spacing are based on single measurements for each colony; when a new interior bud is present, these values represent the distance between the new bud (≤12 septa) and an adjacent mature corallite (24 septa). Values of maximum spacing are also based on single measurements. An interesting relationship was observed between minimum and maximum intercorallite spacing in certain colonies depending on whether a newly
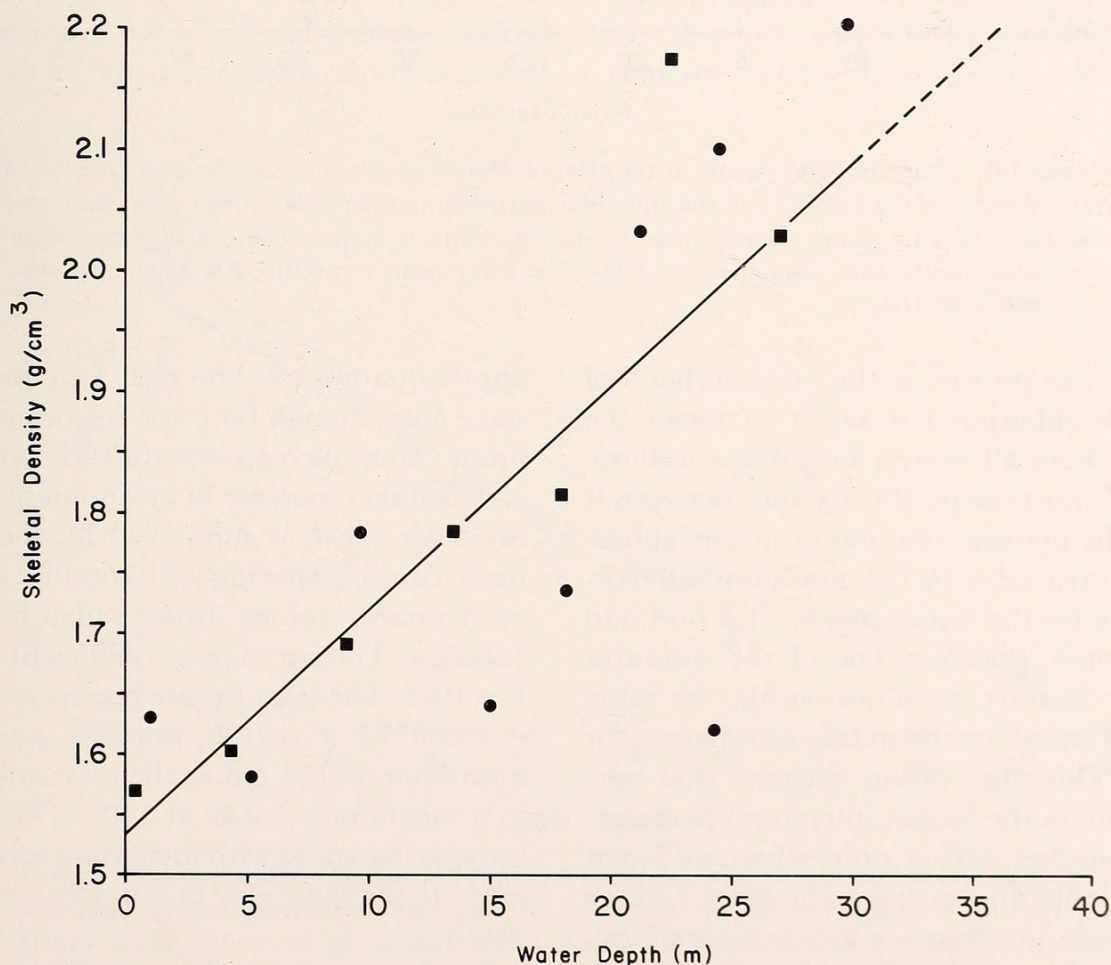

FIGURE 188.—Skeletal density as a function of water depth for colonies of *Montastrea annularis* (circles = single-value data from Carrie Bow Cay, squares = depth-specific averages from St. Croix (Baker and Weber, 1975); regression equation is $Y = 0.0184X + 1.5336$; linear correlation coefficient, $r = 0.790$, $P < 0.01$).
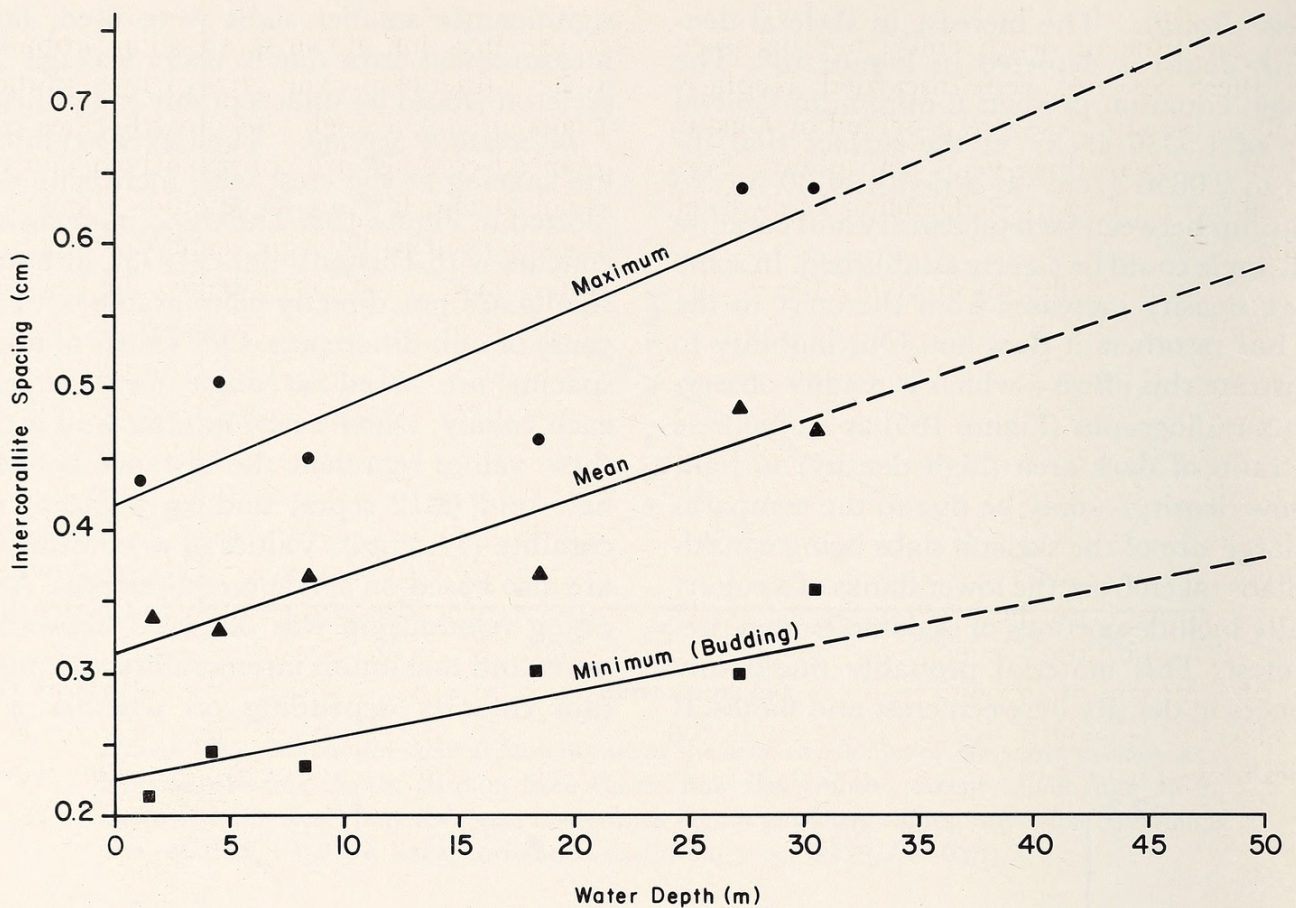
FIGURE 189.—Intercorallite spacing at the crest of *Montastrea annularis* colonies as a function of water depth; similar trends of linear equations for minimum (squares), mean (triangles), and maximum (dots) spacing suggests that interior budding is a space-controlled phenomenon (correlation coefficients: minimum, $r = 0.950$, $P < 0.01$; mean, $r = 0.916$, $P < 0.01$; maximum, $r = 0.866$, $P < 0.05$).

erupted bud was present in the neighborhood of corallites. Neighborhood is taken to mean the area that encloses all nearest neighbor corallites. If a new bud was present, the distance between it and one of the mature corallites in this neighborhood would invariably be the minimum intercorallite spacing for the entire region. If a bud had not yet erupted, however, one of the distances between two mature corallites within the same neighborhod would be the maximum spacing for the region. This observation suggests that new buds originate in the largest intercorallite spaces, and that budding occurs only when sufficient space is available (that is, when the space exceeds a certain maximum distance between corallites). According to the calculated trend lines of Figure 189, this distance criterion is met when the ratio of maximum/minimum intercorallite spacing is

approximately 1.9. This ratio remains nearly constant even though both the maximum and minimum values increase significantly with depth.

The linear increase in mean intercorallite spacing with depth is mimicked by the increase in mean corallite spacing with corallite growth angle on Dustan's colony from a depth of 5 m off Jamaica. The correlation coefficient is $r = 0.888$, $P < 0.01$. The least square regression equation, $Y = 0.00077X + 0.3136$, predicts spacing to be a minimum of 0.31 cm at the crest and to increase to a maximum of 0.42 at 140°. Thus, intercorallite spacing varies with increasing corallite growth angle in the same way that it does with increasing depth.

TRANSPLANTATION EXPERIMENTS.—Deep-water colonies of *Montastrea annularis* transplanted to a depth of 1 m died before they could be collected.

Because the time of death could not be ascertained, these colonies were discarded. Replacements for these samples were provided by Dustan who lent us two three-year transplants from depths of 45 m to 15 m on Dancing Lady Reef, Jamaica.

All transplanted colonies surviving the experiment showed growth modifications of the type and degree expected for in situ colonies at the depths of transplantation. Figure 190 shows the changes in maximum skeletal growth rate among the transplanted specimens. Where the depth of transplantation exceeds the depth of origin, the maximum growth rate decreases, the new rate being in proportion to the new depth; where the depth of transplantation is less than the depth of origin, the maximum growth rate increases in similar fashion. The growth rates of transplanted colonies moved from 1 to 14 m are approximately the same as the growth rates of colonies moved from 45 to 15 m. Thus, the depth of origin as well

as the direction of transplantation probably have little influence on the growth rate at the transplant site. Although the growth rates of transplanted colonies are consistently below the predicted trend for in situ colonies, this result may not necessarily be significant. Colonies 1, 4, 5, and 8 have growth rates below the trend at their depth of origin, so it is not surprising to find them below it at the depth of transplantation. The maximum value of colony 3 could not be measured at the crest owing to nail damage of the polyps, which had to regenerate before normal growth could ensue (Figure 192a). Also, all colonies may have experienced a lag in growth during a period of shock immediately following the transplantation. This period of shock has been observed in other transplant experiments (Dustan, 1975) and may have contributed to the demise of our transplants from deep to shallow water. Colony 8, which was rotated (turned over) 65° and cemented at the same depth, grew at about the
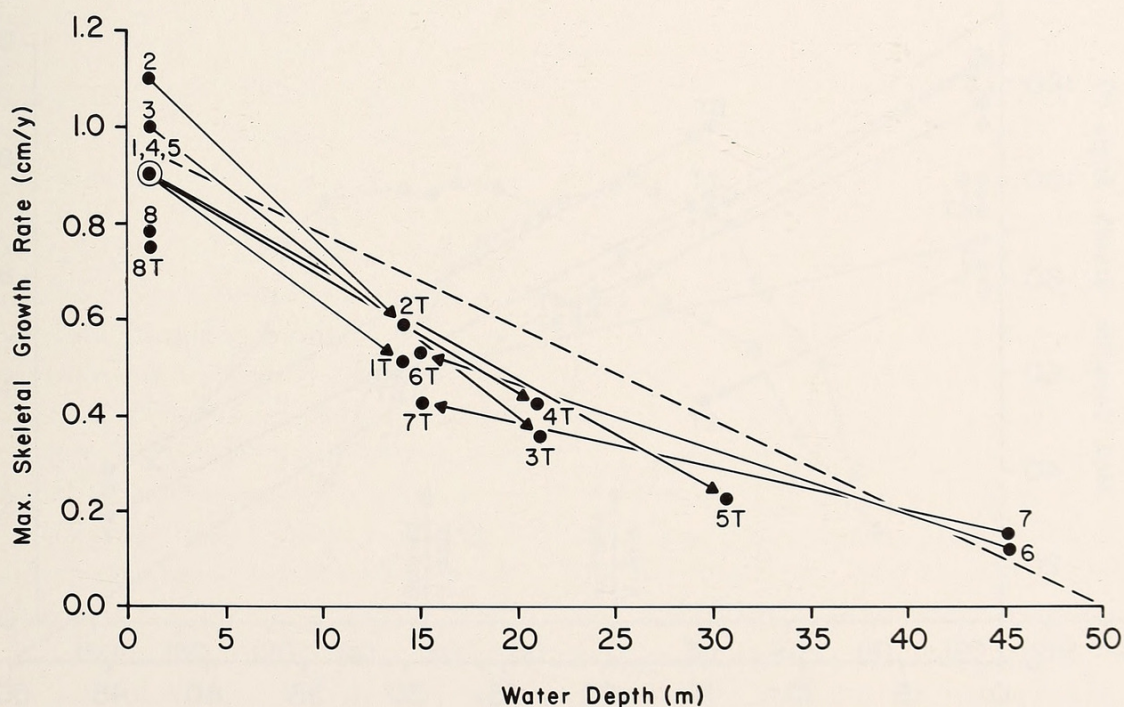

FIGURE 190.—Systematic changes in maximum skeletal growth rate at the crest for colonies of *Montastrea annularis* reciprocally transplanted for 3 years at different depths; solid lines with arrows indicate direction of transplant and change in growth rate over transplant interval; colony 8 was cemented in rotated position (65° to original orientation) at the same depth; colonies 6, 7 are from 3-year transplant data from Jamaica (courtesy P. Dustan); dashed line is the regression equation of the maximum skeletal growth rate vs. depth of in situ colonies (Figure 186).

same maximum rate at the new crest as it had at the old crest.

Changes in maximum angle of corallite growth among the transplanted corals are depicted in Figure 191. Where the depth of transplantation exceeds the depth of origin, colonies have a reduced angle of growth almost proportional to the depth of transplantation. This reduction is caused by a gradual die-back of peripheral polyps (Figure 192a). On the other hand, colonies transplanted to shallower depths show an increase in maximum corallite angle, which is caused by peripheral budding from the epitheca (Figure 192b,c). The colonies may be said to be developing flanks, and given enough time they would probably become tapered hemispheres.

The rotated colony shifted its entire annual growth pattern approximately 65° in the direc-

tion of the new vertical axis (Figure 193). New polyps appearing on the left periphery resembled those in colonies transplanted from deep to shallow water. No die-back occurred at the right periphery but the growth rate was considerably reduced.

Similar reorientation of growth pattern following rotation is evident in an accidentally overturned colony found by David L. Meyer in Panama (Figure 194). After being overturned, the crest shifted to the new vertical position, new polyp growth extended the lower left flank, and polyps on the right flank died back. Polyps on the left side of the new crest accelerated their growth whereas polyps on the right side decelerated their growth. Polyps between the old and new crest developed a sigmoid growth path after their position changed from being on the left of the old
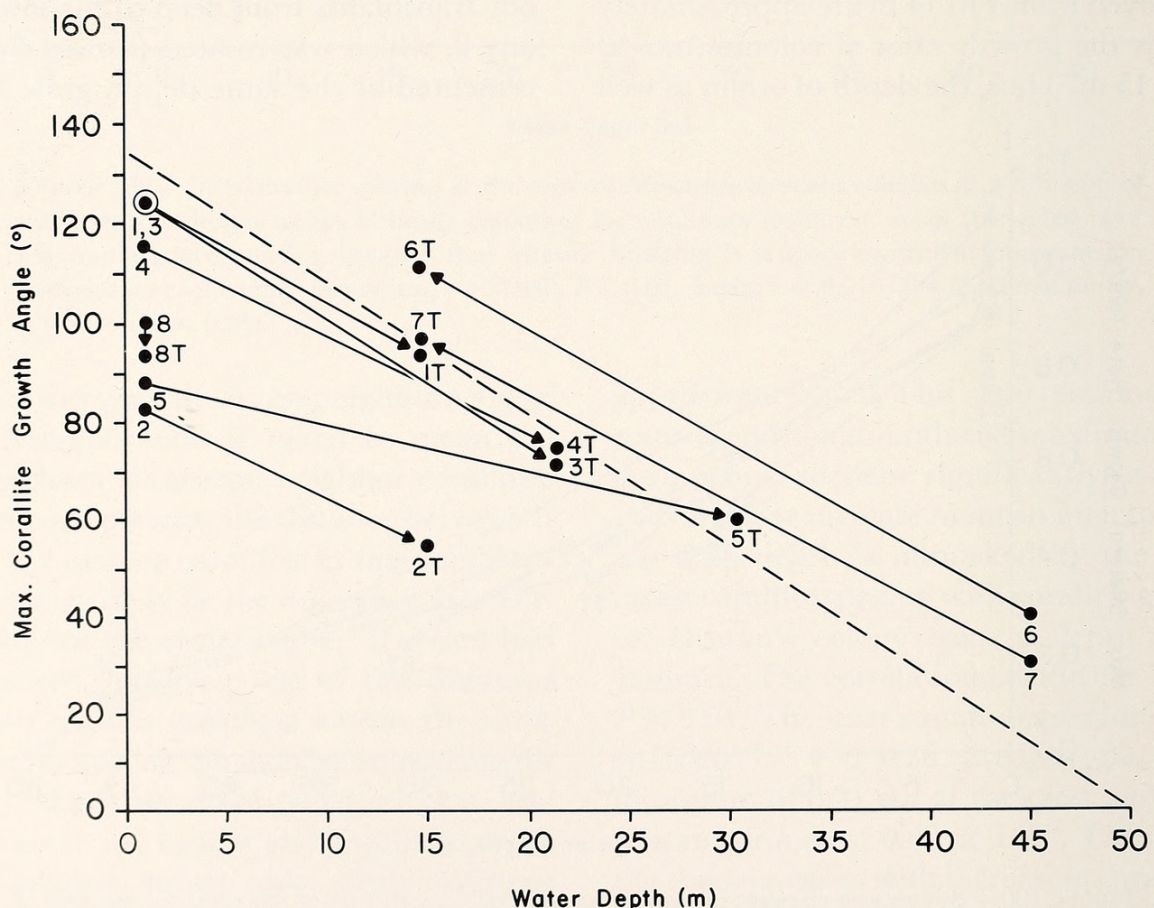

FIGURE 191.—Systematic changes in maximum corallite growth angle (with respect to vertical) for reciprocally transplanted colonies of *Montastrea annularis*; all data from Carrie Bow Cay transect except colonies 6 and 7, which were transplanted off Jamaica; for the rotated colony 8, 8T is the angle relative to the new crest; dashed line is the same regression equation for in situ colonies (Figure 187).

crest to the right of the new crest.

Transplantation-induced changes also took place in skeletal density and corallite spacing. Colonies moved to deeper water showed a significant increase in density at all growth angles (Figure 192a). Conversely, colonies transplanted to shallower water showed a marked decrease in skeletal density for all angles (Figure 192b,c).

FIGURE 192.—Growth pattern alterations in x-radiographs of *Montastrea annularis* colonies after 3 years at transplant site: a, colony 3 (Figures 190, 191), transplanted from 1 m to 20 m off Carrie Bow Cay, shows die-back of live growth surface, reduction of annual growth rate at all corallite angles, and increase in skeletal density; b and c, colonies 6 and 7 (Figures 190, 191), transplanted from 45 m to 15 m off Jamaica, show increase in maximum growth angle, increase in skeletal growth rate, decrease in skeletal density, and decrease in intercorallite spacing due to proliferation of interior buds (arrowhead = position of maximum growth angle before transplant; dot = maximum growth angle 3 years after transplant).
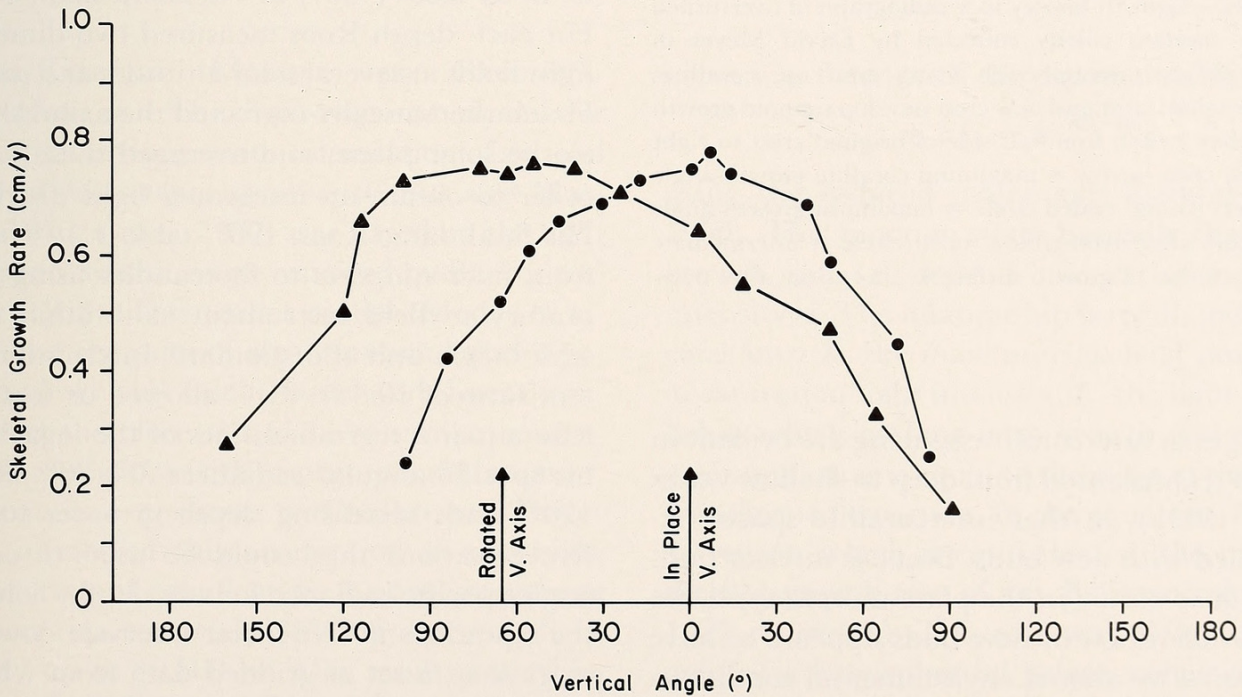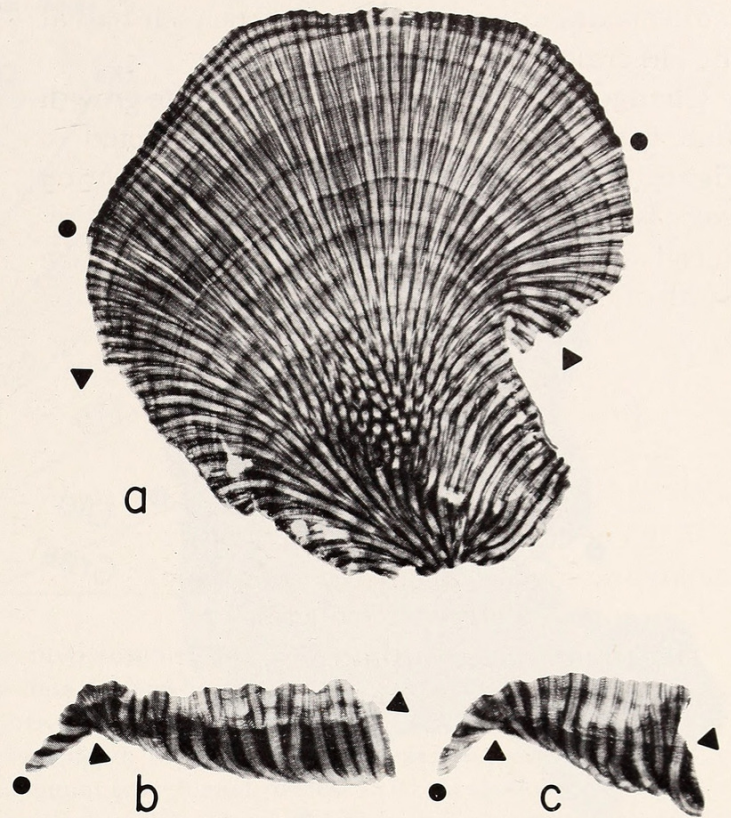
FIGURE 193.—Change in profile of average annual skeletal growth rate with respect to vertical angle for rotated colony 8 (water depth 1 m) 3 years before transplant (dot-plotted curve) and 3 years after transplant (triangle-plotted curve); after transplant, maximum skeletal growth rate remains constant, while maximum growth angle increases about 60° on left side but does not change on other side; vertical distance between curves is a measure of increase or decrease in growth rate at various locations on colony surface (vertical arrows mark positions of original and rotated vertical axes).
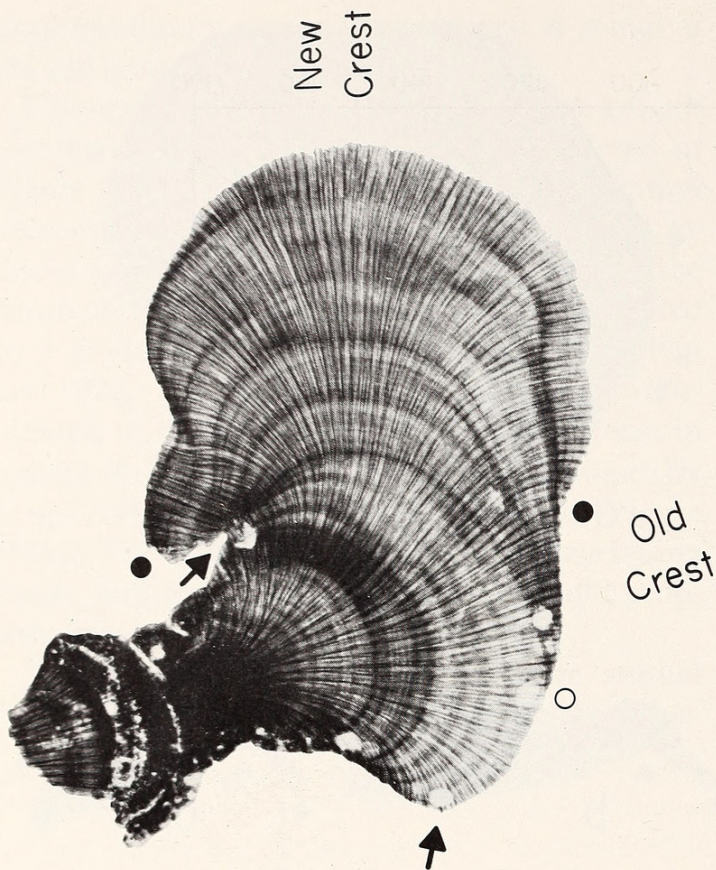
FIGURE 194.—Growth history in x-radiograph of overturned *Montastrea annularis* colony collected by David Meyer in Panama, colony oriented with living crest up; corallites between original crest and new crest develop sigmoid growth paths as they switch from left side of original crest to right side of new crest (arrow = maximum corallite growth angle before overturning; closed circle = maximum growth angle several years after overturning; open circle = intermediate die-back position of growth surface at short time after over-turning).

Changes in intercorallite spacing are evident in material transplanted from deep to shallow water (Figure 192b,c), in that intercorallite spaces become filled with new buds. Because interior budding seldom occurs in the plate morphotype, the rapid proliferation of new buds appears to have been caused by altered environmental conditions at the shallower depth. Despite the decrease in spacing at the crest, spacing at the flanks—which grow at higher angles—remains greater. Changes in intercorallite spacing are difficult to observe in colonies moved from shallow to deep water (Figure 192a), but in general the corallites continue to diverge without further budding as the growth surface expands. Budding would occur eventually, but probably at a set of wider corallite spacings.

These transplant experiments show that the morphological parameters that vary with depth and angle for in situ colonies are the same ones that undergo modification when colonies are moved between depths and allowed enough time to equilibrate with the new environment. The remarkable consistency with which transplanted colonies come to resemble in situ colonies at the same depth strongly suggests that these morphological parameters and the overall growth form are ecophenotypically controlled. Because the pattern of morphological variation closely matches the pattern of variation of submarine light distribution, the most likely factor governing this ecophenotypic response is light.

UNDERWATER RADIANCE DISTRIBUTION.—Data on underwater radiance used in the computer simulation program were derived from open-water measurements made at depths of 5, 10, and 20 m by Roos (1967) in Piscadera Baai, Curaçao. For each depth Roos measured two-dimensional light fields at several solar altitudes and azimuths. He mathematically corrected the azimuthal data to the solar plane, and averaged these values in order to obtain an integrated light distribution. His final data (Roos, 1967, table 11)—converted from microamperes to footcandles using his laboratory to field instrument calibration ratio of 12.5 lx/μA and the standard International System ratio of 10.8 lx/fc — allowed us to compute least squares regression lines of the logarithms of his specific angular radiances (0°, 30°, 60°, 90°, 120°) with increasing depth in order to obtain five equations that could be used to calculate angle-specific radiance for any depth. Solution of the equations at five-meter intervals down to 45 m gave us a set of gridded data from which the contour map in Figure 195 was manually generated. Considering the angular limits of the original data, contours at angles greater than 120° are based on extrapolations and should be interpreted with caution. However, because this portion of the contour map is seldom used in our simulation program, it has not been problematic.
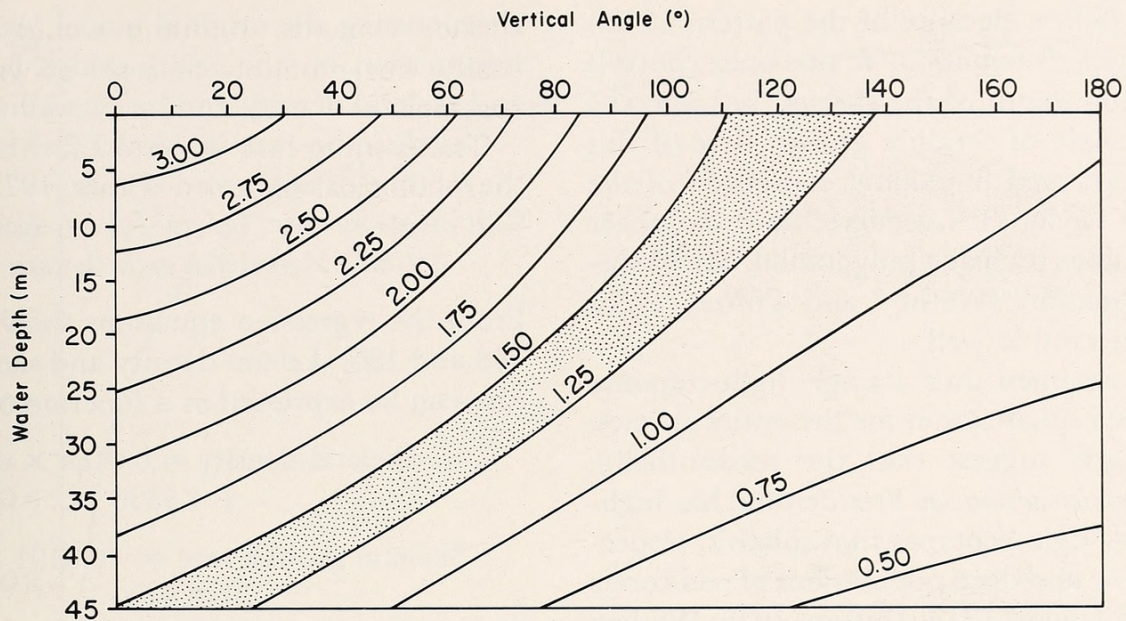
Vertical Angle (°)

FIGURE 195.—Logarithm (base 10) of radiance in footcandles contoured with respect to water depth and angle from the vertical, radiance data derived from Roos (1967, table 11). The dotted area is the range of vertical radiance between 45 m, the reported maximum depth of occurrence, and 50 m, the predicted maximum depth of occurrence of *Montastrea annularis* (Figures 186, 187). In this depth range, the maximum growth angle is close to 0°. At shallower depths the same radiance exists at greater vertical angles, where it defines the maximum corallite growth angle.

LIGHT-RESPONSE MODELS FOR CALCIFICATION.—*Model 1:* The light-response model for calcification in our previous simulation of skeletal growth of *Monstastrea annularis* (Graus and Macintyre, 1976; Graus, 1977) was based on the light and carbon dioxide curve reported by Barnes and Taylor (1973). This earlier model (Model 1) assumed that the rates of algal symbiont photosynthesis and skeletal calcification were linearly related and therefore would have similar mathematical expressions with respect to light intensity. A subsequent experiment by Chalker and Taylor (1975) supported this assumption in observing that the rate of calcification in *Acropora palmata* increases proportionately with subsaturating light intensity up to 10,500 lx. This result, according to the authors, "agrees with studies of photosynthetic carbon fixation in hermatypic corals" (p. 328). Despite this qualitative agreement, however, the quantitative relationship between the rate of photosynthesis and the rate of calcification still remains uncertain.

In our model, the Barnes and Taylor (1973)

curve was fitted with the exponential function

$$r = R[1 - e^{-k(I-Ic)}]$$

using the reduced major axis method (Imbrie, 1956). This function states basically that skeletal growth rate, r, depends on variation in light intensity, I. The relationship is regulated by three constants: R, the maximum skeletal growth rate at saturation light intensity; Ic, the light intensity below which no long-term growth occurs; and k, a constant that is equal to the slope of the linearly transformed equation. In the equation, R is set at 1.1 cm/y, which is equivalent to the maximum skeletal growth rate of any Belizean colony (pre-1975 collection). This rate was measured at the crest of a hemispherical colony collected from a depth of 1 m. The value of Ic was set at 29 footcandles (1 fc = 10.8 lx = 1.6 $\mu W/cm^2$) which corresponds to the vertical radiance at 45 m (extrapolated from light data of Roos, 1967). This depth is considered to be the normal maximum depth of the species (Goreau and Wells, 1967) and is close to the maximum depth for *Montastrea*

annularis in Belize. Because of the pattern of underwater light distribution, I_c not only controls the maximum depth of the species, but also the maximum angle of corallite growth. Use of this equation permitted functional expression of the Barnes and Taylor (1973) curve; however, other fitting equations such as a polynomial, Michaelis-Mention equation (Wethey and Porter, 1976) could have served as well.

Model 1 assumed that a single light-response curve governs calcification for the entire species. Recent reports suggest that the zooxanthella, *Gymnodinium microadriaticum* Freudenthal has highlight and low-light ecotypes that inhabit, respectively, shallow and deep populations of reef corals (Barnes and Taylor, 1973; Dustan, 1975; Wethey and Porter, 1976). If the photosynthetic response mechanism of these ecotypes is indeed distinct, there may also be different light-mediated calcification curves; however, any calcification differences between shallow and deep-water populations have yet to be demonstrated experimentally.

Model 1 also assumed that skeletal growth rate in cm/y is proportional to calcification rate in g/cm²/y. This assumption is correct if the average density of the skeleton is constant. Information about systematic density variations was not available before 1975, but since that time various workers (Baker and Weber, 1975; Dustan, 1975; Highsmith, 1979; and this paper) have shown that average skeletal density increases proportionately with depth and probably with corallite growth angle and therefore is apparently dependent on light intensity.

Model 2: Although light-mediated photosynthesis and calcification are known to be related (Vandermeulen et al., 1972), the biological mechanism and the mathematics of the interaction are still conjectural. Because acceptance of Model 1 depends on the outcome of this continuing discussion, we decided to propose an independent empirical model for calcification in relation to light (hereafter referred to as Model 2; see Appendix for summary of computer program) based on our skeletal measurements of in situ colonies of *Montastrea annularis* from Carrie Bow Cay. In restructuring the original model, we added new information on the relationships between light and skeletal density and intercorallite spacing.

Calcification rate in Model 2 is calculated by the method of Baker and Weber (1975) as follows:

$$\text{Calcification rate (g/cm}^2\text{/y)} = \text{skeletal density (g/cm}^3\text{)} \times \text{skeletal growth rate (cm/y)} \quad (1)$$

From the regression equations shown in Figures 188 and 186, skeletal density and skeletal growth rate can be expressed as a function of depth:

$$\text{Skeletal density} = 0.0184 \times \text{depth} + 1.5336 \quad (2)$$

$$\text{Skeletal growth rate} = -0.0191 \times \text{depth} + 0.9739 \quad (3)$$

A least squares regression of the logarithm (Ln) of mean vertical radiance with depth in Curaçao (Roos, 1967, table 11) gives the following linear equation:

$$\text{Depth} = \frac{7.4696 - \text{Ln (Radiance)}}{0.08881} \quad (4)$$

Sequential substitution of the equations (4) → (3), (2) → (1) yields calcification rate in terms of light intensity. This relationship, plotted in Figure 196, shows how average calcification rate at the crest of the colony declines with attenuation of vertical radiance.

Although this model is derived from morphological measurements, use of it does not predetermine the growth form of a simulated colony. It merely establishes the skeletal growth rate at the crest of a colony at any given depth. Growth rates for corallites in other orientations, and hence the growth form of the colony, depend upon the radiance distribution at the prescribed depth.

Figure 197 shows that the light-response curves for Model 1 and Model 2 are similar in overall shape but differ in detail. Both the maximum growth rate and the minimum light intensity for growth are greater for Model 1 than for Model 2.

SIMULATION EXPERIMENTS.—*Morphotypic Variation with Water Depth:* Model 2 simulations of colony growth of *Montastrea annularis* from depths
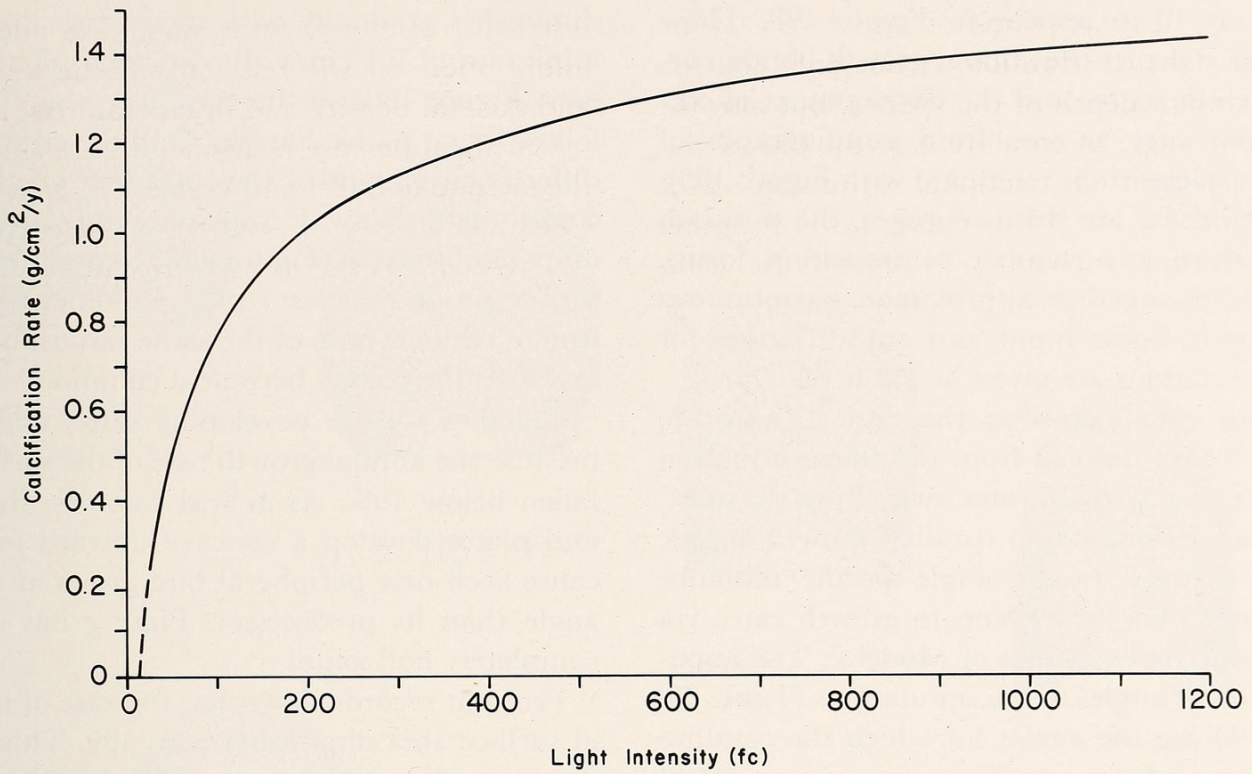
FIGURE 196.—Calcification rate for *Montastrea annularis* as a function of light intensity used in Model 2 computer simulations; curve derived from liner equations fit to empirical mesurements of maximum skeletal growth rate, skeletal density, and light in relation to depth (Figures 186, 188).
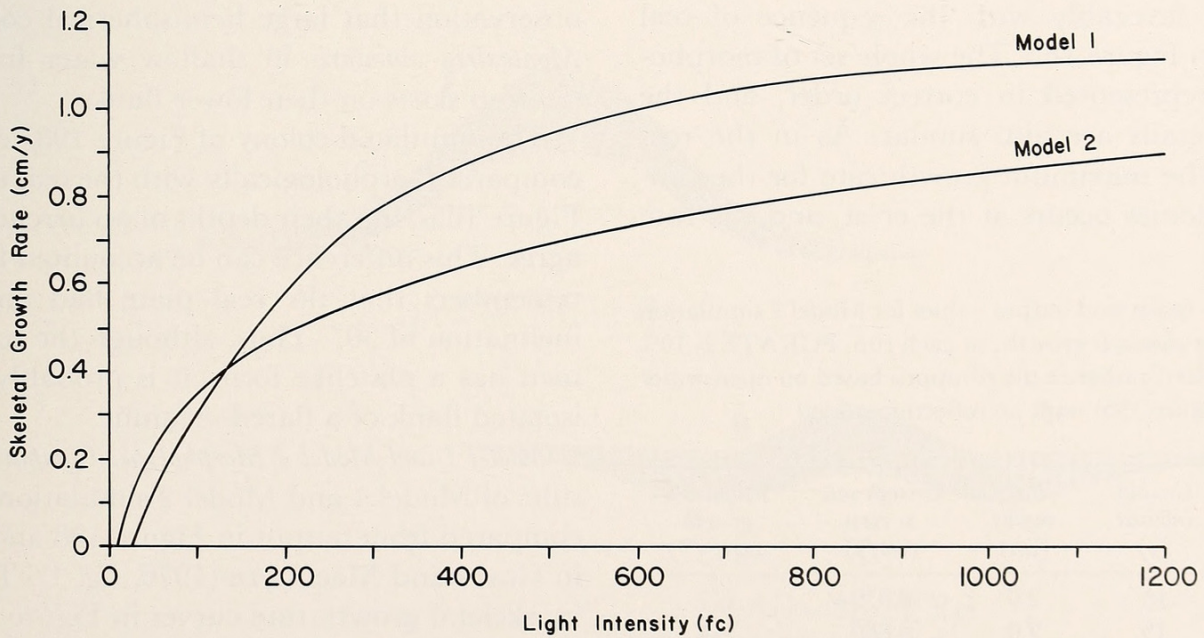

FIGURE 197.—Comparison of Model 1 and Model 2 skeletal growth rate curves in relation to light intensity. Minimum light intensity of long-term growth for 1 is 29 footcandles; for 2 it is 19 fc. Maximum growth rate asymptote for 1 is 1.1 cm/y; for 2 it is 0.9739 cm/y. Curves intersect where light intensity is 135 fc and skeletal growth rate is 0.4 cm/y. Vertical distance between curves is the difference in skeletal growth rate at that light intensity.

of 1 m to 40 m appear in Figure 198. These simulations depict the annual growth bands, corallite growth paths, and the development of corallum geometry as seen from x-radiographs of vertical skeletal slabs (compare with Figure 185). Although these are distinct stages, the program can produce any number of transition forms, which, taken together, approximate a continuous distribution. Some input and output values for these simulations are given in Table 35.

Growth rate values at the crest (Table 35, column 3) are derived from the linear equation in Figure 186. Growth rates away from the crest, as well as the maximum corallite growth angles, depend entirely on the angle-specific radiance values and their conversion to growth rates via the parametric equations of Model 2. The maximum growth angles in the simulations (Table 35, column 4) are the angles for which the corallite growth rate is 0.1 cm/y. These angles correspond closely to values predicted by the regression equation (Figure 187) for real colonies growing at the same depths. This outcome lends independent support for Model 2.

The sequence of simulations in Figure 198 compares favorably with the sequence of real colonies in Figure 185. The whole set of morphotypes is represented in correct order, and the growth details are also similar. As in the real colonies, the maximum growth rate for the simulated colonies occurs at the crest, and the rate

TABLE 35.—Input and output values for Model 2 simulation of *Montastrea annularis* growth; in each run, PGRATE is 10% (see Appendix); radiance distributions based on open-water data (see Figure 195) with no reflection added

Water depth (m)	Growth interval (y)	Base radius (cm)	Growth rate at crest (cm/y)	Maximum growth angle (°)
1	15	2.0	0.959	117
5	15	2.0	0.869	114
10	15	2.0	0.795	97
20	25	2.0	0.587	82
30	10	5.0	0.408	61
35	15	8.0	0.304	45
40	20	8.0	0.204	24

diminishes gradually with increasing angle to a minimum of 0.1 cm/y. In the hemispheric colonies (Figure 198a–c) the corallites near the crest follow linear paths. Farther from the crest, where differential growth of the surface is greater, the corallites curve away from the crest. In the column morphotype (Figure 198d) corallite curvature begins in the crest region. Colonies a–d begin from a circular base of the same radius, but only in d does the colony become a column.

Colonies e–g are developing skirts and plates because the annual growth rate of the surface has fallen below 10%. As in real colonies, the skirts and plates develop a concave upward form because each new peripheral bud grows at a lower angle than its predecessor. Plate g has become completely horizontal.

Printout records show that the rate of increase in surface area diminishes annually. This means that once the rate falls below 10%, it will continue to force, at an ever increasing rate, the growth of the skirt or plate. Even the hemispheric corals will, in time, develop skirts and plates. We estimate that this should happen after about 25–30 years of growth. This conclusion agrees with the observation that large hemispherical colonies of *Montastrea annularis* in shallow water frequently develop skirts on their lower flanks.

The simulated colony of Figure 198g evidently compares morphologically with the real colony of Figure 185e, but their depths of occurrence do not agree. This difference can be accounted for if one remembers that the real plate had an in situ inclination of 30°. Thus, although the real specimen has a platelike form, it is probably just an isolated flank of a flared column.

Model 1 and Model 2 Morphotypes Compared: Results of Model 1 and Model 2 simulations can be compared from output in Figure 198 and output in Graus and Macintyre (1976, fig. 1). The light vs. skeletal growth rate curves in Figure 197 also show the expected outcome. Whenever light intensity exceeds 135 fc (the intersection point of the two curves), skeletal growth rate is greater for Model 1; conversely, whenever it falls below 135 fc the rate is greater for Model 2. According to
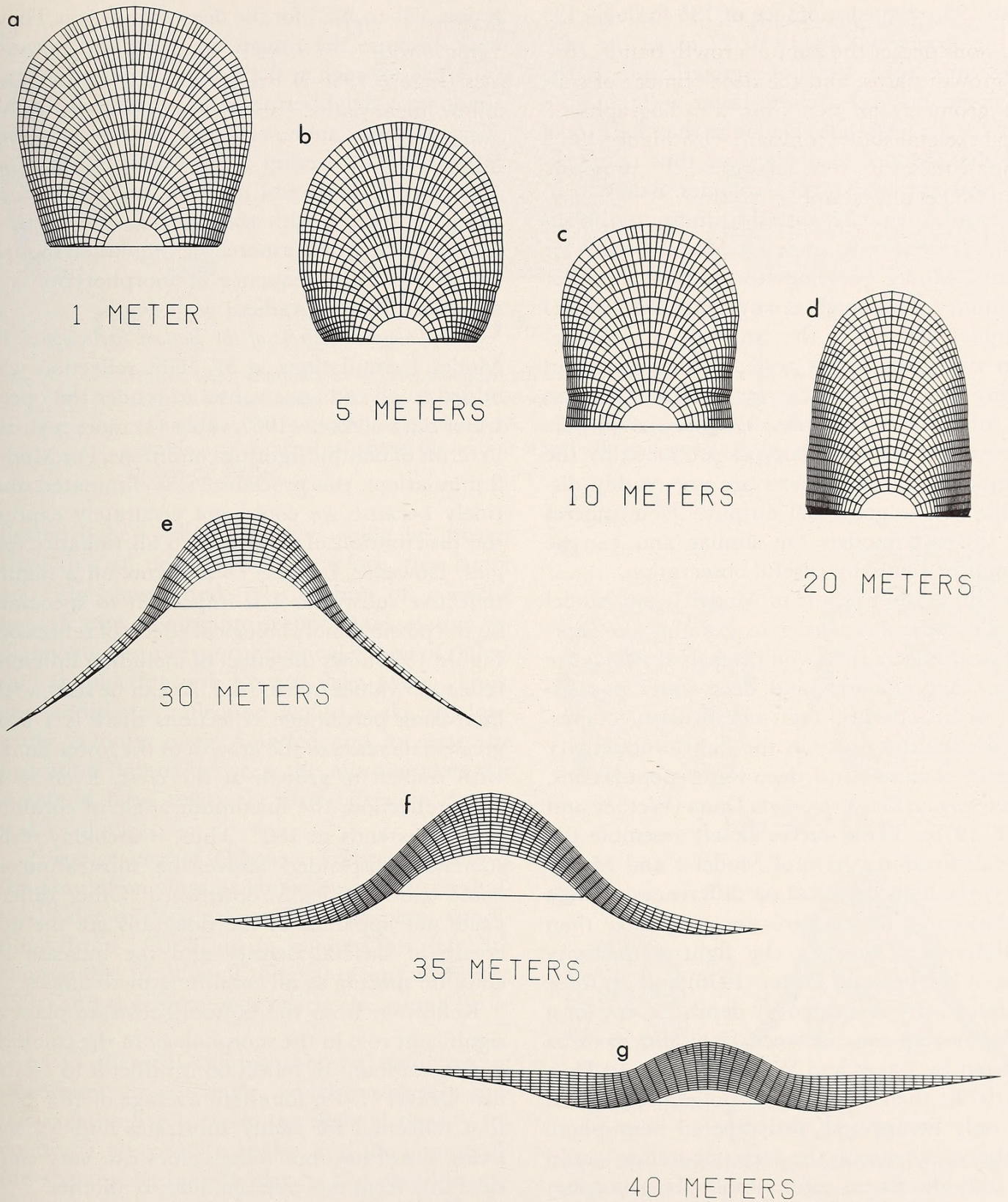
FIGURE 198.—Computer simulation plots of the growth of *Montastrea annularis* colonies in relation to submarine radiance distribution from depths of 1 m to 40 m, generally reproducing the depth-related morphotypic gradient shown in Figure 185; simulations utilize the calcification-light relationship of Model 2 in Figure 196 and open-water radiance data from Roos (1967, table 11) contoured in Figure 195.

Figure 195, vertical radiance of 135 fc ($\log_{10}$ 135 = 2.13) occurs at a depth of 27 m on the reef. Above this depth, then, the growth rate at the crest is greater and declines faster with corallite growth angle for Model 1 colonies than for Model 2 colonies. Model 1 colonies are thus relatively more peaked than Model 2 colonies. Below 27 m the reverse is true. Because the minimum threshold light intensity is lower for Model 2 than for Model 1, Model 2 colonies always have a greater maximum growth angle at any depth than Model 1 colonies. Therefore the transition depths between morphotypes as well as the maximum growing depth are greater for Model 2 colonies than for Model 1 colonies. Despite measurable differences in the morphotypes produced by the two models, the differences are not readily discernible in the graphical outputs. Hemispheres from the two models are similar and can be distinguished only by careful observation.

The simulation results of Model 1 and Model 2 were compared in order to examine the morphological effects that would result if *Montastrea annularis* had shallow- and deep-water populations with separate light-calcification curves. Such a situation exists in the light-productivity curves of shallow- and deep-water populations, respectively, of *Pavona praetorta* Dana (Wethey and Porter, 1976). These curves closely resemble the light-calcification curves of Model 1 and Model 2. If (1) the light-calcification differences of these populations of *M. annularis* are no greater than the differences between the light-productivity curves of Wethey and Porter (1976) and (2) these populations are separated by depth, except for a narrow overlap zone between 15 m and 20 m, as suggested by Baker and Weber (1975) and Dustan (1979), then the shallow population would have only hemisphere and tapered hemisphere morphotypes, whereas the deep population would have only the flared column and plate morphotypes. In the overlap zone, the column morphotype could predominate for both populations. According to the simulation models, these column morphotypes of the two populations would be distinguished by the range of maximum corallite growth angle: 82° to 92° for the shallow popu-

lation, 98° to 108° for the deep population. However, because the ranges are close and because other factors such as slope, bottom reflection, and shading by neighboring organisms also influence the maximum angle, recognizing the two populations in the overlap zone would be difficult. Therefore shallow and deep populations cannot be distinguished with certainty on the basis of growth form. Furthermore, the simulation models suggest that the sequence of morphotypes is a single continuous gradient with depth.

Morphological Effects of the Bottom Reflection: In Model 1 simulations, a 5% light reflection was added to all radiance values to render the open-water data of Roos (1967, table 11) more realistic in terms of benthic lighting conditions. For Model 2 simulations, this procedure was eliminated routinely because we could not accurately express the distribution of reflection to all radiance angles. However, because corals grow on a highly reflective substrate, it is important to speculate on the possible morphological effects of reflection. Figure 199 shows the effect of including different reflection values in Model 2. As can be seen, with increasing percentage reflections there is a progressive increase in the growth of the lower flanks with respect to growth at the crest. Even with 2.5% reflection, the maximum angle of corallite growth extends to 180°. Thus, if a colony were somehow suspended above the substratum it could grow vertically downward. Other differences not apparent in the diagrams are the decrease in skeletal density and the increase in corallite spacing at all corallite growth angles.

Reflection from the bottom substrate plays a significant role in the morphology of the colonies but the amount of reflection is difficult to establish. Brakel (1979) found an average of 18% bottom reflection for sandy substrates and 5% for living substrates, but these values can vary considerably from one microhabitat to another.

The morphological effects of reflection are probably greater for shallow-water colonies than for deep-water colonies. If we consider two colonies, one shallow and one deep exposed to the same percentage reflection (for example, 5% of penetrating light), the amount of additional re-
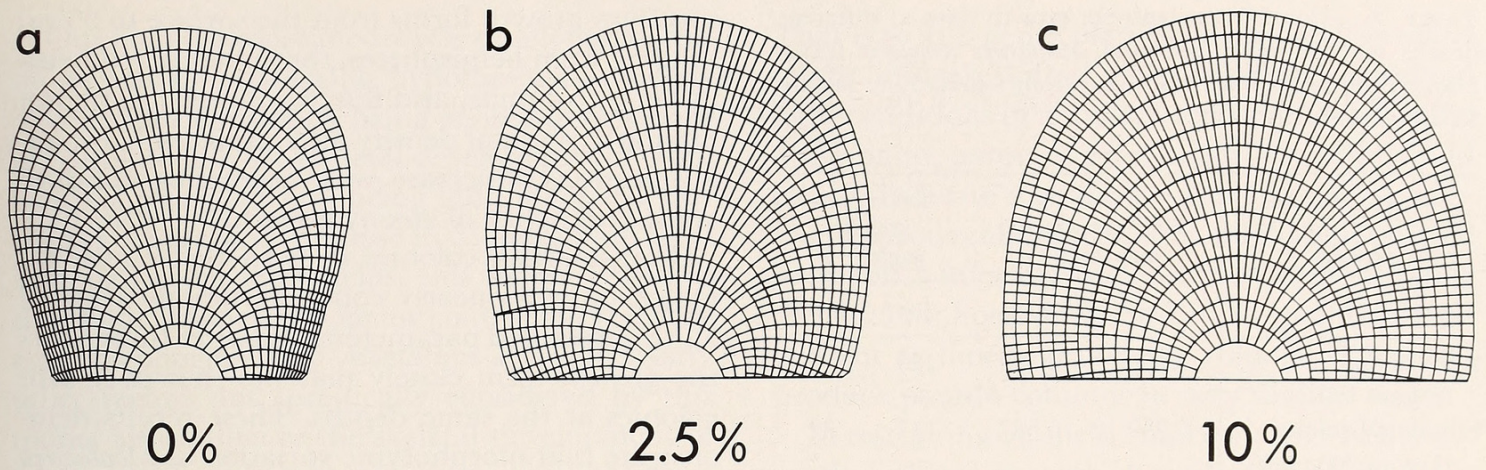
FIGURE 199.—Simulations of morphological effects on colony at 1 m depth resulting from the addition of increasing amounts of light reflection (from bottom substrate) to open water radiance data: *a*, no addition; *b*, plus 2.5%; *c*, plus 10%. Growth increments that include reflection are obtained by adding the percent of vertical radiance equally to radiance values at all vertical angles.

flected light in shallow water would be greater than that in deep water. Therefore, this factor and the postulated relationship of corallite growth rate to absolute rather than relative radiance suggest the morphological effects of reflection should diminish toward deep water. Thus, any additional reflection would make shallow-water colonies more rounded and increase the transition depths between the morphotypes but it should have relatively little effect on deeper water colonies.

Transplantation of Colonies: Figure 200 shows the simulation of transplanted colonies from shallow water to deep water. The transplant conditions (from 1 to 20 m) in Figure 200*a*, left, are comparable to those of the real colony in Figure 192*a*, and the outcome is nearly the same (Table 36).

As in the real colony, there is reduction of maximum growth angle, which involves a dieback of the live surface, the skeletal density increases at all corallite angles, and the intercorallite spacing becomes wider as the corallites diverge without producing interior buds. Figure 200*a*, right, shows an extension of the experiment to 9 years at the transplant site. The transplanted colony has grown a skirt. Although skirt development on a real transplanted colony has not been observed, we would expect it to occur in a natural experiment of this duration. Figure 200*b*
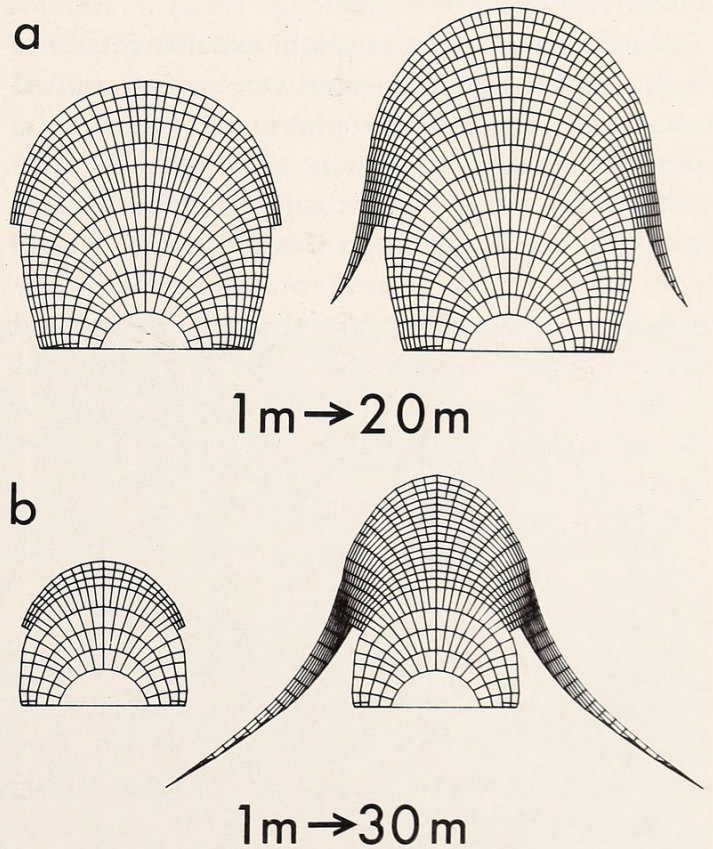

FIGURE 200.—Simulations based on Model 2 showing 3 years (left) and 9 years (right) of growth in shallow to deep water transplant experiments: *a*, transplanted from 1 m to 20 m; *b*, from 1 m to 30 m. As in actual transplant experiments, simulated transplanted colonies experience reductions in growth rate and maximum corallite growth angle proportional to transplant depth, and increases in skeletal density and intercorallite spacing. After 3 years at transplant depth, simulated colonies begin to develop skirts (not observed in actual colonies.)

TABLE 36.—Comparison between growth data at different depths for real and simulated *Montastrea annularis* transplanted colonies; both transplants from 1 m to 20 m lasting for three years

Specimen	Maximum growth rate (cm/y)		Maximum growth angle (°)	
	1 m	20 m	1 m	20 m
Real colony 3 (Figure 192a)	1.000	0.390	125	78
Simulated colony (Figure 200a left)	0.959	0.587	117	82

shows the same type of simulation experiment for a 1 m to 30 m transplanted colony. Comparison of the simulation output (Table 35) with those of the real colony 5 (Figures 190, 191) again shows a close similarity of results.

Similar simulated transplant experiments from deep water to shallow water were not attempted because the computer program would have to be modified. We have no doubt they could be done successfully. In addition, it should be possible to simulate the change in growth pattern produced by experimental or natural rotation of the colony (see Figure 194). For this, the program would have to be altered so that it calculates both sides of the colony (at present, because only one half of the colony is calculated, it must be bilaterally symmetrical).

Conclusions

Stained colonies of *Montastrea annularis* and their x-rays have provided a detailed understanding of the major geometric parameters that dicate the growth and morphotypic variations of this species. In all colonies studied, for example, maximum skeletal growth rate occurs in vertically oriented corallites that are usually situated at the crest of the colony and the rate of growth diminishes systematically with corallite growth angle. The maximum growth rate and the maximum vertical angle of corallite growth also diminish linearly with depth. These varying combinations of parameters produce a continuous spectrum of

corallum growth forms from the surface to 50 m, ranging from hemispheres, through tapered hemispheres, columns, and flared columns, to plates. Similarly, skeletal density and intercorallite spacing gradually increase with increasing corallite angle and depth of colony growth.

Transplanted colonies in both Belize and Jamaica undergo nearly complete modification of all the described parameters, and after three years the growth form closely matches that of in situ colonies at the same depths. These results demonstrate that morphotypic variation of *Montastrea annularis* with depth is predominantly an ecologically rather than a genetically controlled phenomenon. A similar conclusion was reached by Foster (1979), who found, using similar transplant experiments, a high degree of phenotypic plasticity in the corallite microarchitecture of this species.

With these new data we were able to construct a computer simulation model to evaluate the relationship between submarine light distribution and the growth forms of *Montastrea annularis*. Unlike our earlier model (Model 1 in Graus and Macintyre, 1976), which was based on experimental studies of photosynthesis and calcification in response to light intensity, this empirical model (Model 2) was based on calcification in relation to light as established by our measurements of skeletal characteristics relative to corallite orientation and water depth.

Simulation experiments with Model 2 show that as in the case of Model 1 a broad range of morphotypes produced are comparable to the corallum growth form sequence observed with increasing depth on the Carrie Bow reef transect. In addition, simulations of the transplant experiments replicate the observed changes in growth forms and show that the modifications result from a combination of altered skeletal growth rate, maximum corallite growth angle, skeletal density, and intercorallite spacing. Simulation experiments on the effects of bottom reflection indicate that variation of the lighting conditions in the microhabitat can significantly alter corallum morphology.

Our light-response model was developed to test quantitatively a working hypothesis, the details of which are constantly being revised as new data are obtained on the skeletal development of tropical reef corals. In producing morphological variations comparable to those in colonies from habitats of known light fields, this model confirms that light is the major factor controlling the skeletal morphogenesis of *Montastrea annularis*. Many other factors not specifically considered by this model also influence the skeletal development of *M. annularis*, such as the symbiotic growth interaction of this coral and the sponge *Mycale laevis* (Goreau and Hartman, 1966).

It should also be noted that ambient light conditions can vary considerably within habitats at the same depth. For example, shallow-water corals growing in shaded microhabitats or on sloping substrates exhibit skeletal (morphogenesis) characteristics normally associated with colonies in deeper water. Such variations in light field and related variations in skeletal characteristics must be taken into account whenever our findings are used to interpret paleoenvironments.

That is to say, dense platy growths of *M. annularis* might indicate either deep water or restricted light conditions in a shallow environment. On the other hand, porous hemispherical growths would clearly indicate a shallow-water habitat. A relatively porous columnar colony might also be used to establish intermediate paleodepths in the range of 15–25 m; however, crowding of colonial development or bioerosion on the colonial flanks can produce pseudo-columns in very shallow water.

In restricting our field observations to relatively small, isolated, smooth-shaped colonies, we have not taken into account variations in shape and colonial architecture of other *Montastrea annularis* colonies within the same reef habitat. For example, in the shallow back-reef area off Ambergris Cay (Figure 201a), one massive development of smooth-surfaced "knobby" (terminology in Dustan, 1975) *M. annularis* has some areas of distinctly "lumpy" surfaces. Although these two surface types have a similar yellow-brown color, the "lumpy" areas have denser skeletons, wider corallite spacings, and greater corallite relief than the "knobby" growths. In the same back-reef
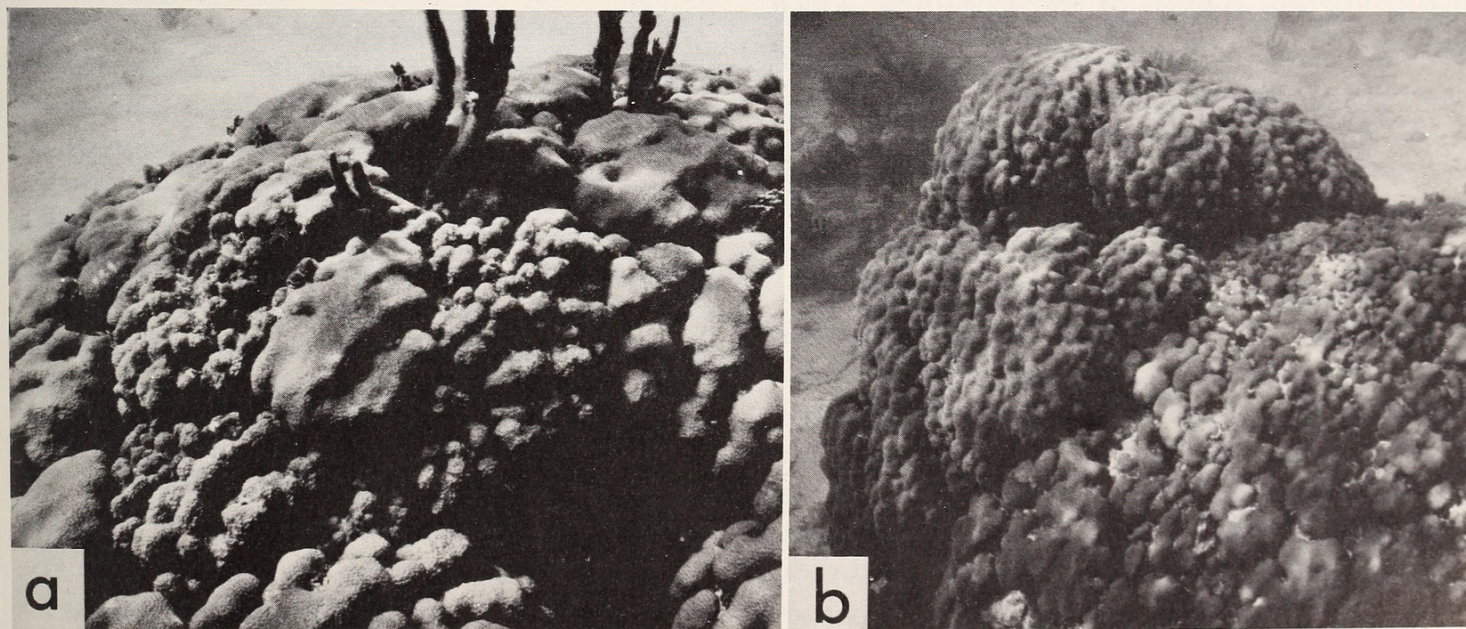

FIGURE 201.—Variations in colonial growth of *Montastrea annularis* in patch reefs in the shallow back-reef area off Ambergris Cay: *a*, large yellow-brown development of *M. annularis* with areas of "lumpy" widely spaced corallites between relatively smooth-surface "knobby" growth; *b*, yellow-brown isolated "knobby" *M. annularis* in the foreground, which contrasts sharply with continuous dark brown surfaces of "lumpy" growth in background.

area, dark brown, "lumpy" *M. annularis* can be found growing in juxtaposition with yellow-brown "knobby" colonies (Figure 201*b*). In the latter case, the colors of the various growth forms differ, although the skeletal density and corallite surface characteristics are similar.

These variations in skeletal morphogenesis—which have been observed in the deeper fore-reef as well as the shallow back-reef areas off Carrie Bow Cay—are still unexplained. The lack of evidence that this skeletal development is a response to ecological conditions suggests that it could be genetically determined.

Appendix

Synopsis of Model 2 Computer Program

The computer program for simulation of growth of *Montastrea annularis* is stored at Museum of Natural History, Smithsonian Institution, and is available by contacting the authors. The program written in FORTRAN IV is divided into two parts: a main program, which performs the substantive calculations, and a plotting program, which generates plotted output on a Calcomp (California Computer Products) plotter. The main program consists of seven routines, which are described below in program order.

1. READ INPUT VARIABLES

External communication with the program is carried out by entering values of the following six variables, which establish the experimental conditions for each simulation run:

NYEARS   numbers of years of growth of simulated colony

RADNCE   sequence of depth-specific radiance values at 5° intervals from 0° (up) to 180° (down)

REFL   percent of vertical radiance from bottom substrate to be added to all radiance values

PGRATE   minimum allowable annual increase in colony surface area

RBASE   radius of circular base of simulated colony

TPLANT   transplant switch that tells the program to grow the colony using two different sets of radiance data, one at the origin depth and one at the transplant depth

2. CALCULATE ANGLE-SPECIFIC ANNUAL GROWTH INCREMENTS

The 5° RADNCE values are first linearly interpolated to obtain values at 1° intervals, and the entire radiance distribution is then smoothed using the three point moving average method. The light values for all angles are then converted into annual growth increments by the sequence of parametric equations of Model 2. The maximum growth angle is set at the angle for which the annual growth increment equals 0.1 cm/y. This corresponds with the observation that if a polyp survives a year, it will grow at least at that rate.

3. ESTABLISH COLONY BASE AND INITIAL CORALLITE POSITIONS

The simulated colony starts growing on a circular base of radius, RBASE. Although a circle adequately approximates the shape of an early growth stage of a colony, the program can be easily modified to accept basal coordinates from a real specimen. The base is positioned so that its center is on the *Y*-axis at or near origin of the rectangular coordinate system. The *Y*-axis is also the vertical symmetry axis of the colony. The negative *Y*-quadrant is not displayed; thus, the *X*-axis is the flat bottom substrate.

The terminus of the first corallite is placed at the intersection of the circular base with the Y-axis, and is assigned a corallite growth angle of $0°$, thereby establishing its orientation perpendicular to the base. The location of the second corallite is then placed on the perimeter in the positive X,Y quadrant, 1.5 times the minimum budding distance (IPDIST) from the first corallite. Its corallite growth angle, also perpendicular to the base, is the angle between vertical and a radius drawn from the center of the circle to the coordinates of the second corallite. Additional corallites are positioned in the same manner, relative to the previous corallite, until the maximum growth angle is reached.

4. CALCULATE NEW GROWTH SURFACE AND CORALLITE POSITIONS

The colony grows beyond the base in yearly or other regular events up to the number specified by NYEARS. Corallite growth angles are first converted into annual growth patterns by adding the various calculated annual growth increments to the terminal positions of the corallites in the directions specified by the growth angles. These projected coordinates define the next annual growth surface of the colony.

The corallites cannot be extended merely to the new surface, however, because most of them would violate the rule that they grow perpendicular to that surface. To solve this problem, the correct path of a corallite to the new growth surface is determined by calculating a perpendicular line from the previous corallite position to a line segment extending between the projected coordinates of flanking corallites. The growth increment is then adjusted to correspond with the new growth angle.

5. CALCULATE COLONY SURFACE AREA

In computing the live surface area, the colony is assumed to be a radially symmetric solid of revolution with a vertical axis of symmetry. Horizontal sections cut through the colony connecting the coordinates of the corallites divide the colony into a series of trapezoidal solids. The sum of the external surface areas of these trapezoidal segments is the total living surface area of the colony. The area of the new growth surface is calculated and then compared with the area of the previous growth surface. If the increase exceeds the minimum growth rate specified by PGRATE, program control transfers to the interior budding routine; if not, the program control transfers to the peripheral budding routine below.

6. PERIPHERAL BUDDING

Peripheral budding occurs only when the annual increase in surface area falls below the minimum value specified by PGRATE. In this routine, a new bud is added at a distance 1.5 $\times$ IPDIST from, and at a growth angle $3°$ less than, that of the terminal corallite. The growth angle of the new bud is prevented from becoming less than $0°$. After addition of the new bud, the total surface area is recomputed and compared with the area of the previous growth surface. If it still falls below the required minimum, new buds are added one at a time until the test is passed

7. INTERIOR BUDDING

An interior bud is generated whenever the distance between adjacent corallites exceeds the maximum intercorallite spacing, IPDIST $\times$ 2.0. The new bud is positioned midway between flanking corallites at a growth angle that bifurcates the angle between those corallites.

8. PLOTTING PROGRAM

After the entire colony is calculated by the main program, yearly growth events are plotted one at a time using the stored coordinates of the corallites. The growth surface is drawn first by connecting the X,Y coordinates in order from the vertical to the terminal corallite, with the plotting pen held down on the paper. Next, the axes of the corallites are drawn by connecting the coordinates of corallites on the new growth surface to the coordinates of those same corallites on the previous growth surface. Then, the X-coordinates of all the corallites are reversed, and the mirror image of the half-colony is plotted in the $-X,Y$ quadrant.

Literature Cited

Baker, P. A., and J. A. Weber
  1975. Coral Growth Rate: Variation with Depth. *Earth and Planetary Science Letters*, 27:57–61.

Barnes, D. J., and D. L. Taylor
  1973. In Situ Studies of Calcification and Photosynthetic Carbon Fixation in the Coral *Montastrea annularis*. *Helgoländer Wissenschaftliche Meeresuntersuchungen*, 24:284–291.

Brakel, W. H.
  1979. Small-Scale Spatial Variation in Light Available to Coral Reef Benthos: Quantum Irradiance Measurements from a Jamaican Reef. *Bulletin of Marine Science*, 29(3):406–413.

Chalker, B. E., and D. L. Taylor
  1975. Light-Enhanced Calcification, and the Role of Oxidative Phosphorylation in Calcification of the Coral *Acropora cervicornis*. *Proceedings, Royal Society of London*, series B, 190:323–331.

Dustan, P.
  1975. Genecological Differentiation in the Reef-Building Coral *Montastrea annularis*. 300 pages. Ph.D. dissertation, State University of New York, Stony Brook.
  1979. Distribution of Zooxanthellae and Photosynthetic Chloroplast Pigments of the Reef-building Coral *Montastrea annularis* (Ellis and Solander) in Relation to Depth on a West Indian Coral Reef. *Bulletin of Marine Science*, 29(1):79–95.

Foster, A. B.
  1979. Phenotypic Plasticity in the Reef Corals *Montastrea annularis* (Ellis and Solander) and *Siderastrea siderea* (Ellis and Solander). *Journal of Experimental Marine Biology and Ecology*, 39:25–54.

Goreau, T. F., and W. D. Hartman
  1966. Sponge: Effect on the Form of Reef Corals. *Science*, 151(3708):343–344.

Goreau, T. F., and J. W. Wells
  1967. The Shallow-Water Scleractinia of Jamaica: Revised List of Species and Their Vertical Distribution Range. *Bulletin of Marine Science*. 17:442–453.

Graus, R. R.
  1977. Investigation of Coral Growth Adaptations Using Computer Modeling. *In* D. L. Taylor, editor, *Proceedings of the Third International Symposium on Coral Reefs*, 2:463–469. Miami, Florida: Rosenstiel School of Marine and Atmospheric Science.

Graus, R. R., and I. G. Macintyre
  1976. Light Control of Growth Form in Colonial Reef Corals: Computer Simulation. *Science*, 193(4256):895–897.

Highsmith, R. C.
  1979. Coral Growth Rates and Environmental Control of Density Banding. *Journal of Experimental Marine Biology and Ecology*, 37:105–125.

Imbrie, J.
  1956. Biometrical Methods in the Study of Invertebrate Fossils. *Bulletin of American Museum of Natural History*, 108:211–252.

Macintyre, I. G., and S. V. Smith
  1974. X-Radiographic Studies of Skeletal Development in Coral Colonies. *In* A. M. Cameron et al., editors, *Proceedings of the Second International Coral Reef Symposium*, 2:277–287. Brisbane, Australia: Great Barrier Reef Committee.

Roos, P. J.
  1967. Growth and Occurrence of the Reef Coral *Porites astreoides* Lamarck in Relation to Submarine Radiance Distribution. Ph.D. dissertation, Drukkerij Elinkwijk, Utrecht, 72 pages.

Vandermeulen, J. H., N. Davis, and L. Muscatine
  1972. The Effect of Inhibitors of Photosynthesis on Zooxanthellae in Corals and Other Marine Invertebrates. *Marine Biology*, 16:185–191.

Wethey, D. S., and J. W. Porter
  1976. Sun and Shade Differences in Productivity of Reef Corals. *Nature*, 262(5566):281–282.